J|A|C|S ARTICLES

Published on Web 07/06/2009

Introduction of Methionines in the Gas Channel Makes [NiFe] Hydrogenase Aero-Tolerant

Sébastien Dementin,[†] Fanny Leroux,[†] Laurent Cournac,[‡] Antonio L. de Lacey,[§] Anne Volbeda,[||] Christophe Léger,[†] Bénédicte Burlat,[†,⊥] Nicolas Martinez,[||] Stéphanie Champ,[†] Lydie Martin,[||] Oliver Sanganas,[#] Michael Haumann,[#] Víctor M. Fernández,[§] Bruno Guigliarelli,[†,⊥] Juan Carlos Fontecilla-Camps,[||] and Marc Rousset*[,†]

CNRS, Bioénergétique et Ingénierie des Protéines, IMM, 31 Chemin Joseph Aiguier, 13402 Marseille Cedex 20, France, CEA Cadarache, DSV, IBEB, Laboratoire de Bioénergétique et Biotechnologie des Bactéries et Microalgues, UMR 6191 CNRS/CEA/ Aix-Marseille Université, 13108 Saint-Paul-lez-Durance, France, CEA Grenoble, DSV, IBS (CEA, CNRS, UMR5075, Université Joseph Fourier), Laboratoire de Cristallographie et de Cristallogenèse des Protéines, 41 rue Jules Horowitz, 38027 Grenoble Cedex 1, France, Aix-Marseille Université, 3 place Victor Hugo, 13331 Marseille Cedex 3, France, Instituto de Catalisis, CSIC, c/ Marie Curie 2, 28049 Madrid, Spain, and Freie Universität Berlin, FB Physik, Arnimallee 14, 14195 Berlin, Germany

Received March 19, 2009; E-mail: rousset@ifr88.cnrs-mrs.fr

Abstract: Hydrogenases catalyze the conversion between $2H^+ + 2e^-$ and H_2[1]. Most of these enzymes are inhibited by O_2, which represents a major drawback for their use in biotechnological applications.[1,2] Improving hydrogenase O_2 tolerance is therefore a major contemporary challenge to allow the implementation of a sustainable hydrogen economy. We succeeded in improving O_2 tolerance, which we define here as the ability of the enzyme to resist for several minutes to O_2 exposure, by substituting with methionines small hydrophobic residues strongly conserved in the gas channel. Remarkably, the mutated enzymes remained active in the presence of an O_2 concentration close to that found in aerobic solutions in equilibrium with air, while the wild type enzyme is inhibited in a few seconds. Crystallographic and spectroscopic studies showed that the structure and the chemistry at the active site are not affected by the mutations. Kinetic studies demonstrated that the inactivation is slower and reactivation faster in these mutants. We propose that in addition to restricting O_2 diffusion to the active site of the enzyme, methionine may also interact with bound peroxide and provide an assisted escape route for H_2O_2 toward the gas channel. These results show for the first time that it is possible to improve O_2-tolerance of [NiFe] hydrogenases, making possible the development of biohydrogen production systems.

1. Introduction

Hydrogenases are the key enzymes of hydrogen metabolism. They catalyze the reversible heterolytic cleavage of molecular hydrogen according to the reaction: $H_2 \leftrightarrow 2H^+ + 2e^-$.[1] These metallo-enzymes are classified as [NiFe] and [FeFe] hydrogenases according to the metal content of their binuclear active site.[3] They are widely distributed among micro-organisms and are involved in a variety of important energy-generating processes in which hydrogen is consumed or evolved.[4] These processes occur mainly in anaerobic biotopes, because most hydrogenases are very sensitive to O_2 inhibition. As a result, in the vast majority of microorganisms, the expression of hydrogenase genes is repressed under aerobiosis.[4]

[NiFe] hydrogenases that have been inactivated upon prolonged exposure to O_2 can be reactivated,[1,5] whereas [FeFe] hydrogenases are usually irreversibly damaged.[1,6] A few examples of relatively O_2-tolerant [NiFe] hydrogenase have been reported, including the membrane-bound hydrogenase (MBH) or the soluble hydrogenase (SH) from the Knallgas bacterium *Ralstonia eutropha*,[7] the hydrogenases from *Aquifex aeolicus*[8] and a hydrogenase from *Rubrivivax gelatinosous*.[9] However, the O_2-tolerant enzymes tend to be less active than the prototypical [NiFe] enzymes which are O_2-sensitive.[3] Another group of hydrogenase-like enzymes, highly O_2-tolerant but even

[†] CNRS, Bioénergétique et Ingénierie des Protéines.
[‡] CNRS/CEA/ Aix-Marseille Université.
[§] Instituto de Catalisis, CSIC.
[||] CEA, IBS, Grenoble.
[⊥] Aix-Marseille Université.
[#] Freie Universität Berlin.

(1) De Lacey, A. L.; Fernandez, V. M.; Rousset, M.; Cammack, R. *Chem. Rev.* **2007**, *107*, 4304–4330.
(2) Rousset, M.; Cournac, L. In *Bioenergy*; Wall, J. D., Harwood, C. S., Demain, A., Eds.; ASM Press: Washington D.C., 2008; pp 249–257.
(3) Fontecilla-Camps, J. C.; Volbeda, A.; Cavazza, C.; Nicolet, Y. *Chem. Rev.* **2007**, *107*, 4273–4303.
(4) Vignais, P. M.; Billoud, B. *Chem. Rev.* **2007**, *107*, 4206–4272.
(5) Vincent, K. A.; Parkin, A.; Armstrong, F. A. *Chem. Rev.* **2007**, *107*, 4366–4413.
(6) Baffert, C.; Demuez, M.; Cournac, L.; Burlat, B.; Guigliarelli, B.; Bertrand, P.; Girbal, L.; Leger, C. *Angew. Chem., Int. Ed.* **2008**, *47*, 2052–2054.

 10.1021/ja9018258 CCC: $40.75

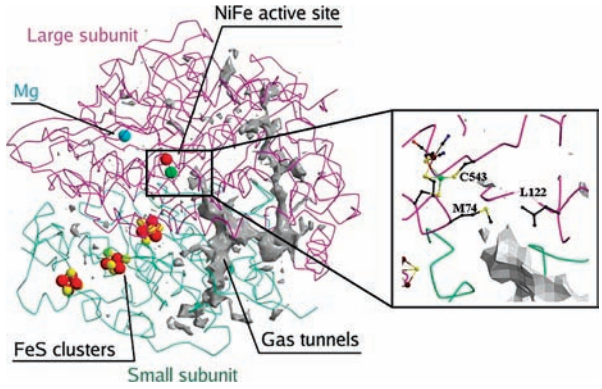

Figure 1. Crystallographic structure of the [NiFe] hydrogenase from *D. fructosovorans* at 1.8 Å resolution (PDB: 1YQW). The gas channel network is depicted in gray. It was calculated with a probe radius of 0.8 Å. The position of the methionine in the V74M mutant (PDB: 3H3X) is indicated in the inset.

less active, collects the H_2-sensors such as the RH from *Ralstonia eutropha*[10] and the HupUV proteins from *Rhodobacter capsulatus*[11] and *Bradyrhizobium japonicum.*[12]

Biotechnological applications would benefit from using these O_2-tolerant hydrogenases in H_2 photoproduction processes or in biofuel cells. However, it is very difficult to produce active [NiFe] hydrogenases in heterologous hosts because the maturation machinery is host-specific.[13] Improving O_2 resistance of hydrogenases in micro-organisms selected for bioprocesses is therefore a major challenge. With this aim in view, the study of the molecular bases of O_2-tolerance of these hydrogenases represent precious inspiration sources.

In [NiFe] hydrogenases, a channel network allows gas diffusion between the protein surface and the active site[14] (Figure 1). At the end of the hydrophobic channel of O_2-sensitive hydrogenases, near the Ni−Fe site, two conserved hydrophobic residues, most commonly valine and leucine, are replaced by isoleucine and phenylalanine, respectively, in the O_2-tolerant H_2-sensors.[15] Thus it has been hypothesized that increasing the bulk of the residues occupying these two positions may reduce the channel diameter, thereby impeding O_2 access to the active site.[15] This "molecular sieve" hypothesis was seemingly supported by the observation that I/F to V/L mutations in H_2-sensors increased their O_2 sensitivity.[16,17]

Our aim in this work was to study the molecular bases of oxygen sensitivity in [NiFe] hydrogenases using the abundant, structurally resolved, and genetically modifiable *Desulfovibrio fructosovorans* enzyme as a model system. Based on the molecular sieve hypothesis, we have explored the role of the two conserved amino acids at the end of the gas channel in the resistance to O_2. We show that the replacement of valine and leucine (V74 and L122 in *D. fructosovorans*) by isoleucine and phenylalanine does not afford O_2 tolerance. Subsequently, we have introduced at these positions two methionines, inspired by their role in oxidative stress responses[18−20] or by the affinity of their sulfur atom for oxygenated species.[21] We show that methionines allow the enzyme to remain catalytically active when exposed to an O_2 concentration similar to that in air-equilibrated solutions. The recombinant hydrogenases exhibit a slower rate of aerobic inactivation and a faster rate of reactivation than the wild type.

2. Materials and Methods

2.1. Bacterial Strains, Plasmids and Growth Conditions. Cells were grown under conditions described in ref 14.

2.2. Site-Directed Mutagenesis. The QuikChange XL site-directed mutagenesis kit (Stratagene, Amsterdam, The Netherlands) was used to generate point mutations in the large *hynB* subunit. The subcloning strategy and the controls are described in ref 14.

2.3. Protein Purification. The tagged recombinant hydrogenases were purified on a Strep-Tactin column (IBA Gmbh), as described previously.[22] One additional purification step using Q-sepharose column (Amersham Biosciences, Uppsala, Sweden) was performed. The purification yields of the recombinant M74/M122 hydrogenases were 0.7 to 1 mg of pure enzymes per liter of culture.

2.4. H^+/D^+ Exchange Reaction. H^+/D^+ exchange in aqueous phase was monitored continuously by a membrane-inlet mass-spectrometric method[23] at 30 °C in a 1.5 mL vessel containing 50 mM phosphate buffer, pH 7. Prior to measurements, hydrogenase was activated by incubation under an H_2 atmosphere in the presence of 100 μM methyl viologen (MV). Anoxia of samples during activation was easily monitored by the blue color of reduced MV. The assay was then performed in the following way: D_2 was bubbled into the medium in the vessel until O_2 was decreased to the desired concentration, the vessel was then closed and an aliquot of activated hydrogenase (20 μL of activated sample, representing 1 to 2.5 μg of enzyme) was injected. Hydrogenase activity was then calculated from the rate of isotopic exchange as described previously,[24] or from D_2 uptake rate when this process occurred.

2.5. EPR Spectroscopy. EPR spectra were recorded on a Bruker ELEXSYS 500E spectrometer fitted with an Oxford Instruments ESR 900 helium flow cryostat. Redox titrations were performed in an anaerobic cell as described previously.[22] For photoconversion studies, the sample was illuminated directly in the EPR cavity through a fiber optic by using a 250 W (Fiberoptic-Heim) quartz lamp.

2.6. Electrochemical Measurements. Protein film voltammetry experiments[25] were performed using the methods and equipment

(7) Burgdorf, T.; Lenz, O.; Buhrke, T.; van der Linden, E.; Jones, A. K.; Albracht, S. P.; Friedrich, B. *J. Mol. Microbiol. Biotechnol.* **2005**, *10*, 181–196.
(8) Guiral, M.; Aubert, C.; Giudici-Orticoni, M. T. *Biochem. Soc. Trans.* **2005**, *33*, 22–24.
(9) Maness, P. C.; Weaver, P. F. *Appl. Microbiol. Biotechnol.* **2001**, *57*, 751–756.
(10) Bernhard, M.; Buhrke, T.; Bleijlevens, B.; De Lacey, A. L.; Fernandez, V. M.; Albracht, S. P.; Friedrich, B. *J. Biol. Chem.* **2001**, *276*, 15592–15597.
(11) Elsen, S.; Colbeau, A.; Chabert, J.; Vignais, P. M. *J. Bacteriol.* **1996**, *178*, 5174–5181.
(12) Black, L. K.; Fu, C.; Maier, R. J. *J. Bacteriol.* **1994**, *176*, 7102–7106.
(13) Casalot, L.; Rousset, M. *Trends Microbiol.* **2001**, *9*, 228–237.
(14) Leroux, F.; Dementin, S.; Burlat, B.; Cournac, L.; Volbeda, A.; Champ, S.; Martin, L.; Guigliarelli, B.; Bertrand, P.; Fontecilla-Camps, J. C.; Rousset, M.; Léger, C. *Proc. Natl. Acad. Sci. U.S.A.* **2008**, *105*, 11188–11193.
(15) Volbeda, A.; Montet, Y.; Vernede, X.; Hatchikian, C. E.; Fontecilla-Camps, J. C. *Int. J. Hydrogen Energy* **2002**, *27*, 1449–1461.
(16) Duche, O.; Elsen, S.; Cournac, L.; Colbeau, A. *FEBS J.* **2005**, *272*, 3899–3908.
(17) Buhrke, T.; Lenz, O.; Krauss, N.; Friedrich, B. *J. Biol. Chem.* **2005**, *280*, 23791–23796.
(18) Stadtman, E. R.; Moskovitz, J.; Berlett, B. S.; Levine, R. L. *Mol. Cell. Biochem.* **2002**, *234−235*, 3–9.
(19) Stadtman, E. R. *Arch. Biochem. Biophys.* **2004**, *423*, 2–5.
(20) Stadtman, E. R. *Free Radic. Res.* **2006**, *40*, 1250–1258.
(21) Pal, D.; Chakrabarti, P. *J. Biomol. Struct. Dyn.* **2001**, *19*, 115–128.
(22) Dementin, S.; Burlat, B.; De Lacey, A. L.; Pardo, A.; Adryanczyk-Perrier, G.; Guigliarelli, B.; Fernandez, V. M.; Rousset, M. *J. Biol. Chem.* **2004**, *279*, 10508–10513.
(23) Jouanneau, Y.; Kelley, B. C.; Berlier, Y.; Lespinat, P. A.; Vignais, P. M. *J. Bacteriol.* **1980**, *143*, 628–636.
(24) Cournac, L.; Guedeney, G.; Peltier, G.; Vignais, P. M. *J. Bacteriol.* **2004**, *186*, 1737–1746.
(25) Léger, C.; Bertrand, P. *Chem. Rev.* **2008**, *108*, 2379–2438.

described in ref.[26] All experiments were carried out with an open electrochemical cell, in a glovebox (Jacomex) filled with N_2 (residual $O_2 < 1$ ppm). The enzymes were adsorbed into a pyrolytic graphite edge rotating electrode, and then fully activated under reducing conditions as described previously.[14] To test the inhibition of the enzyme by O_2, the enzyme-coated electrode was immersed into the electrochemical cell which contained 3 mL of pH 7.0 buffer continuously flushed with pure H_2, rotated at 2,000 rpm, poised at a potential of +200 mV vs SHE. Under these conditions, the hydrogen-oxidation activity is measured as a positive current. Then 500 μL of the same buffer previously equilibrated with air at room temperature was injected in the cell, instantly raising the concentration of O_2 to about 28 μM (assuming that 250 μM of O_2 is dissolved in the aerated buffer). The resulting decrease in current against time revealed the aerobic inactivation of the enzyme: the faster the decrease, the greater the sensitivity. After each injection, O_2 was flushed from the solution by the stream of H_2, and its concentration decreased exponentially with time, with a characteristic time of about 20 s under typical conditions.[26]

2.7. Crystal Structure Determination of the V74M Mutant and Modeling. Crystals of this mutant were obtained and stored in liquid nitrogen as described for the S499A mutant of *D. fructosovorans* [NiFe]-hydrogenase.[15] A total of 180° of diffraction data was collected at 100K on a square ADSC Q315R detector, using for each image a $\Delta\phi$ of 0.7 degrees, an exposure time of 0.5 s and an X-ray wavelength of 0.976 Å at the ID29 beamline of the European Synchrotron Radiation Facility in Grenoble, France. Diffraction spots were integrated, scaled and subjected to a zero-dose correction[27] with XDS.[28] A final data reduction step was performed with the CCP4 package.[29] The crystal structure was refined with REFMAC[30] using a strategy similar to the one described for the S499A mutant,[31] adding noncrystallographic symmetry restraints for the three hydrogenase molecules in the asymmetric unit to compensate for the relatively low data resolution of 2.7 Å. The mutated residue appears to be partially disordered: in the final model the occupations of the Sδ and Cϵ atoms of Met74 were reduced to 80% in each of the three enzyme molecules to prevent the appearance of a negative peak in a 3-fold averaged $F_o - F_c$ map. No alternative conformation could be resolved. Intensity data and refinement statistics are shown in Supplementary Table 1 (Supporting Information). Modeling was carried out as described in ref 31 using TURBO-FRODO.[32]

2.8. FTIR Spectroscopy. The infrared experiments were done in a spectroelectrochemical cell (activation and anaerobic inactivation) as described in ref[33] or in a gastight transmission cell (aerobic inactivation) as described in ref.[34] In the case of aerobic inactivation experiments, the O_2 concentration slowly increases from 0 to 200 μM.

2.9. XAS. Hydrogenase proteins were concentrated to a content of ~1 mM of Ni and ~20 μL were filled into Kapton-covered acrylic-glass sample holders and frozen in liquid nitrogen. XAS at the Ni K-edge was performed at the Synchrotron Radiation Source (SRS) Daresbury (UK) at beamline 16.5 using a double-crystal (Si220) monochromator and a 30-element energy-resolving Ge detector (Ortec) for X-ray fluorescence detection. Samples were held in a liquid-helium cryostat at 20K. After energy calibration of each scan (using reference absorption spectra of a Ni foil measured in parallel to the protein samples), spectra were summed, normalized, and EXAFS oscillations were extracted as described in ref 35. EXAFS spectra were transformed into *k*-space using an E_0 of 8333 eV and Fourier-transforms (FTs) were calculated over a *k*-range of 2−12.5 Å^{-1} using 10% cos^2 windows at both ends. EXAFS simulations were performed with the in-house program SimX[35] using phase functions calculated by FEFF 8.0.[36]

3. Results and Analysis

3.1. Kinetic Characterizations of the Recombinant Enzymes. In the [NiFe] hydrogenase from *D. fructosovorans*, V74 and L122 were substituted by I and F, respectively (FI mutant). Alternatively, methionines were introduced at these positions to construct the V74M mutant, the L122M mutant and the double MM mutant. The mutations introduced in the enzyme did not affect the purification yield. H_2 oxidation activity was determined at 30 °C with 50 mM methyl viologen under 1 atm of H_2.[14] The apparent k_{cat} measured under these conditions are 750 s^{-1} for the WT and the L122M mutant, 800 s^{-1} for the FI mutant, 590 s^{-1} for the MM mutant and 530 s^{-1} for V74M. These activity values suggest that the active sites of the mutants are intact and functional.

3.2. H^+/D^+ Exchange Activity (HDE). To determine hydrogenase activity in the presence of oxygen, we injected purified hydrogenase extracts into an aerobic buffer bubbled with D_2, and monitored by mass spectrometry the changes in concentration of H_2, HD, D_2, and O_2. The inactivation by O_2 of the *D. fructosovorans* WT and FI mutant [NiFe] hydrogenase is almost instantaneous at concentrations around 22 μM (Figure 2A), and neither D_2 uptake nor H^+/D^+ exchange could be observed. In addition, a prolonged incubation under reducing conditions was required for the enzyme reactivation. The L122M mutant behaved as the native enzyme and will not be discussed further (data not shown).

In contrast, the V74M mutant remains active in the presence of an initial concentration of 150 μM O_2, which is demonstrated by the D_2 consumption activity (dashed line in Figure 2B). The decrease of O_2 concentration (red line) is mediated by the reduced methyl viologen (MV) produced by the active hydrogenase (traces of MV are present in the buffer because it is used for activating the enzyme, see Methods). O_2 and D_2 concentrations decrease with a stoichiometry of one D_2 molecule for two O_2 molecules, according to the reactions: $D_2 + 2MV_{ox} \rightarrow 2MV_{red} + 2D^+$ and in the presence of O_2: $2O_2 + 2MV_{red} \rightarrow 2MV_{ox} + 2O_2^-$. As long as O_2 is present, the electron flux is driven toward O_2 reduction, which prevents the exchange reaction (i.e., H_2 and HD production) to occur. The exchange reaction can start when all O_2 has been reduced (Figure 2B, black line). This experiment demonstrates that the V74M mutant remains active during a significant period of time in the presence of O_2 in concentration close to that in an air-equilibrated solution.

(26) Leger, C.; Dementin, S.; Bertrand, P.; Rousset, M.; Guigliarelli, B. *J. Am. Chem. Soc.* **2004**, *126*, 12162–12172.
(27) Diederichs, K.; McSweeney, S.; Ravelli, R. B. *Acta Crystallogr., D: Biol. Crystallogr.* **2003**, *59*, 903–909.
(28) Kabsch, W. In *International Tables for Crystallography*; Kluwer Academic Publishers: Dordrecht, 2001; Vol. F.
(29) Collaborative Computational Project Number 4; *Acta Crystallogr., D: Biol. Crystallogr.* **1994**, *50*, 760–763.
(30) Murshudov, G. N.; Vagin, A. A.; Dodson, E. J. *Acta Crystallogr., D: Biol. Crystallogr.* **1997**, *53*, 240–255.
(31) Volbeda, A.; Martin, L.; Cavazza, C.; Matho, M.; Faber, B. W.; Roseboom, W.; Albracht, S. P.; Garcin, E.; Rousset, M.; Fontecilla-Camps, J. C. *J. Biol. Inorg. Chem* **2005**, *10*, 239–249.
(32) Roussel, A.; Cambillau, C. *The Turbo-Frodo graphics package;* Silicon Graphics Geometry Partners Directory, Vol. 81; Silicon Graphics Corp: Mountain View, CA, 1991.
(33) De Lacey, A. L.; Stadler, C.; Fernandez, V. M.; Hatchikian, E. C.; Fan, H. J.; Li, S.; Hall, M. B. *J. Biol. Inorg. Chem.* **2002**, *7*, 318–326.
(34) Volbeda, A.; Garcin, E.; Piras, C.; de Lacey, A. L.; Fernandez, V. M.; Hatchikian, C. E.; Frey, M.; Fontecilla-Camps, J. C. *J. Am. Chem. Soc.* **1996**, *118*, 12989–12996.
(35) Dau, H.; Liebisch, P.; Haumann, M. *Anal. Bioanal. Chem.* **2003**, *376*, 562–583.
(36) Zabinsky, S. I.; Rehr, J. J.; Ankudinov, A.; Albers, R. C.; Eller, M. J. *Phys. Rev. B: Condens. Matter* **1995**, *52*, 2995–3009.

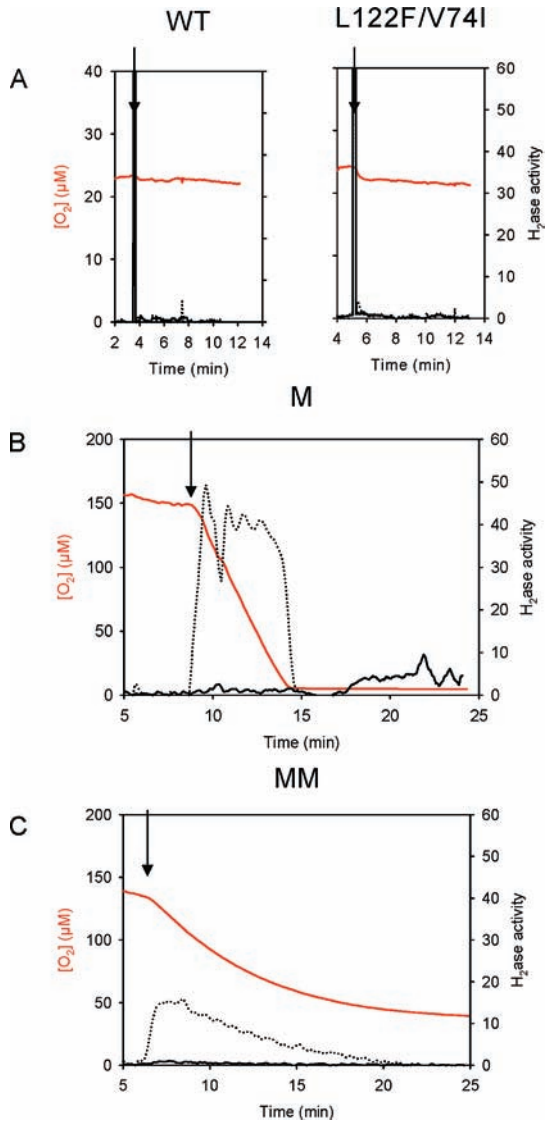

Figure 2. Comparison of the HDE kinetics for the (A) WT and FI, (B) V74M, and (C) MM enzymes in the presence of O_2. The arrow indicates the injection of the activated enzyme (see MM). Red lines: oxygen concentration, black lines: hydrogenase mediated isotope exchange rates, dotted lines: D_2-consumption rate. The hydrogenase activities (exchange or consumption) are expressed in μmol/min/mg.

In the case of the MM mutant (Figure 2C), the enzyme is also active in the presence of 150 μM of O_2, but the kinetics of D_2 consumption and O_2 reduction are slower and vanish during the time course of the experiment. Since the determination of the apparent k_{cat} show that the M and MM mutants oxidize H_2 at similar rates under anaerobic conditions, the lower apparent activity of the MM variant in the presence of O_2 (Figure 2C) likely results from the enzyme being more sensitive to O_2, as confirmed below.

3.3. Protein Film Voltametry (PFV). We also used protein film voltammetry (PFV)[25,26] to discriminate between the mutants on the basis of their sensitivity to O_2. The enzyme is adsorbed onto a graphite electrode which is immersed into a buffer equilibrated under 1 atm. of H_2 and the electrode potential is set to a value that is positive with respect to the reduction potential of the H^+/H_2 couple. The electrons produced upon catalytic oxidation of H_2 are directly transferred from the enzyme to the electrode. This is detected as a current which is proportional to the enzyme's activity and which can be sampled

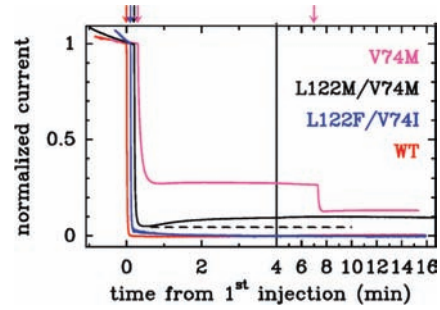

Figure 3. Relative changes in hydrogen-oxidation activity following transient exposure to air, under very oxidizing conditions, monitored by PFV. The vertical arrows mark the injections of 28 μM O_2. The hydrogen-oxidation currents were normalized with respect to the values measured just before the first injection of O_2. $E = 190$ mV vs SHE, 1 atm of H_2. pH 7, 40 °C, electrode rotation rate 2 krpm. The dashed line is a horizontal guide to the eye.

at high frequency to examine the variation of activity that occurs upon exposure to an inhibitor. To test the effect of O_2 on hydrogenase by electrochemistry, the electrode potential must be poised at a value that is high enough so that O_2 is not directly reduced on the electrode surface (this would interfere with the activity measurement and decrease the interfacial concentration of O_2). Under these oxidizing conditions, the enzyme inactivates even in the absence of O_2, as a result of slow anaerobic oxidation.[26,37,38] This, and the slow desorption of the enzyme from the electrode, are the reasons why the current slowly decreases even before O_2 is added (at $t < 0$) in Figure 3. In these experiments, O_2 is flushed away by the stream of H_2 and then removed from the electrochemical cell within a few minutes following the injection.

From the data in Figure 3, we note two major differences between the variants. First, the red and blue lines in Figure 3 show that the WT and FI mutant quickly lose all activity after 28 μM O_2 has been added (idem with 10 μM O_2, data not shown). In contrast, all things being equal, the MM and V74M mutants retain activity after they have been exposed to O_2 (black and magenta lines, respectively). The inactivation stops after the O_2 concentration has dropped to zero, but repeating the injection makes the activity drop again; this is exemplified for the V74M mutant by the magenta line (at $t = 7$ min in Figure 3).

Second, when the MM mutant is exposed to O_2 (black line in Figure 3), the fast inactivation is followed by a partial recovery of activity (from $t = 40$ s to $t = 4$ min), which occurs after the O_2 concentration has dropped back to zero. This is clearly visible in Figure 3 as an upward deviation from the dashed, horizontal guideline. Under the very oxidizing conditions we use, anaerobic inactivation and film loss should provoke a continuous decrease of the current, even in the absence of O_2; hence any increase in current is unexpected and significant. We did not observe this reactivation under oxidizing conditions with the WT enzyme,[26] with the FI mutant, or in control experiments carried with other mutants whose Michaelis Menten constant for H_2 is high (data not shown). This latter observation shows that the increase in current is not the mere consequence of H_2 concentration recovering to that in equilibrium with 1

(37) Jones, A. K.; Lamle, S. E.; Pershad, H. R.; Vincent, K. A.; Albracht, S. P.; Armstrong, F. A. *J. Am. Chem. Soc.* **2003**, *125*, 8505–8514.
(38) de Lacey, A. L.; Hatchikian, E. C.; Volbeda, A.; Frey, M.; Fontecilla-Camps, J. C.; Fernandez, V. M. *J. Am. Chem. Soc.* **1997**, *119*, 7181–7189.

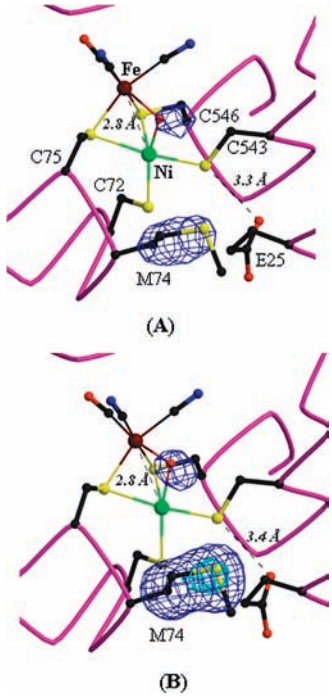

Figure 4. Comparisons of the active sites of *D. fructosovorans* [NiFe] hydrogenase mutants crystallized under air. (A) V74M mutant (PDB: 3H3X), (B) MM mutant (3CUR). The blue grids depict 3-fold averaged $F_{obs} - F_{calc}$ omit-maps contoured at 6σ and calculated at 2.7 and 2.4 Å resolution in (A) and (B), respectively. Ni−Fe and C543Sγ-E25Oϵ1 distances are highlighted.

atm H_2 after the injection. Consistently, we show in reference[39] that this reactivation can be detected with the L122M/V74M mutant even when very small amounts of aerated solnjection. Consistently, we show in referenceutions are injected in the solution (see Figure 5 therein), provided the decrease in current resulting from film loss and anaerobic inactivation is carefully corrected. It is indeed important to note that reactivation can only be detected if it is faster than anaerobic inactivation, since the two reactions have opposite effects on the current. In the case of the M variant, the small but meaningful increase in current seen after O_2 has vanished (magenta line in Figure 3) demonstrates that the chemistry that is responsible for the "reactivation under oxidative conditions" in the MM variant also takes place in V74M, but at a slower rate.

3.4. Crystal Structure Determination. Well-diffracting crystals were obtained for the V74M mutant under aerobic conditions. The overall structure and the cavities of this mutated protein are similar to those of the MM and FI mutants as reported in reference 14. An elongated electron density bridging the Ni and Fe ions (Figure 4A) suggests the presence of a significant Ni-A fraction characterized by a (hydro)peroxide ligand.[31] This density is also observed in the aerobically obtained structure of the MM mutant (Figure 4B). Atomic coordinates and structure factors for the V74M mutant have been deposited in the Protein Data Bank with deposition code 3H3X.

3.5. EPR Spectroscopy. EPR spectroscopy was used to probe the integrity of the metal centers of the mutants in both the oxidized and reduced states. Figure 5A shows that the V74M

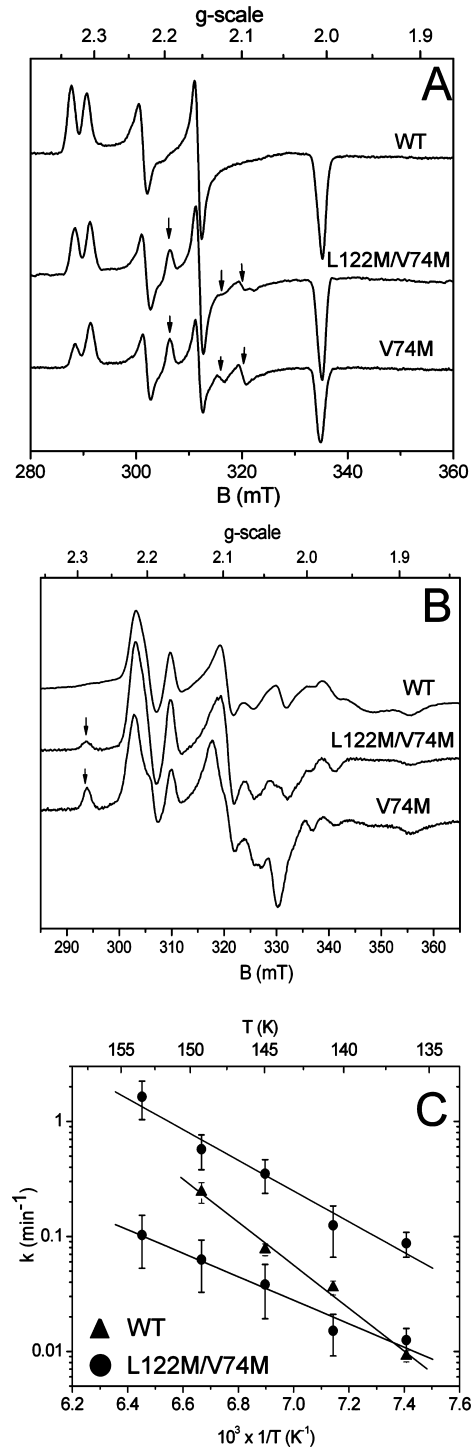

Figure 5. EPR spectra of the NiFe active site in the (A) oxidized and (B) reduced states. Recording conditions: microwave power 10mW, modulation amplitude 1mT, temperature (A) 100 K and (B) 6 K, microwave frequency 9.406 (1) GHz. Arrows in A indicate the position of the peaks at $g = 2.195$ and $g = 2.10$ which are absent in the WT. Arrows in B indicate the position the gz peak of the new species at $g_{z,y,x} = 2.286$, 2.080, and 2.045 which resembles the Ni-L2. (C) Temperature dependence of the kinetics of the Ni-L2 to Ni−C recombination process.

mutant displays identical signatures to those previously observed in the MM mutant.[14] In the oxidized state, the EPR spectrum is dominated by the active site signatures of the Ni-A ($g = 2.31$, 2.23, 2.01) and Ni−B ($g = 2.34$, 2.16, 2.01) species, which are very similar to those of the WT enzyme (Figure 5A). In the V74M and MM mutants, weak additional peaks are observed

(39) Fourmond, V.; Lautier, T.; Baffert, C.; Leroux, F.; Liebgott, P. P.; Dementin, S.; Rousset, M.; Arnoux, P.; Pignol, D.; Meynial-Salles, I.; Soucaille, P.; Bertrand, P.; Leger, C. *Anal. Chem.* **2009**, *81*, 2962–2968.

around $g = 2.19$ and 2.10 and correspond to a small contribution (<15% of the paramagnetic nickel) of the NiFe center. The ratio Ni−B/Ni−A appears to be different in the WT and in the mutants. However, by studying several preparations of "as-prepared" WT hydrogenase, we found that this ratio and the total amount of the paramagnetic Ni greatly vary between preparations. Therefore, no correlation could be established between the ratio of the Ni−B/Ni−A signals measured in the as-prepared state and the oxygen sensitivity of the variants.

Upon reduction of the enzyme, we observed the usual Ni−C species of the active site in both mutants. This is a key intermediate in the catalytic cycle, in which a hydride bridges the Ni and the Fe. The EPR signal intensity of this species shows a bell-shaped variation in a potential range which is similar to that of the WT enzyme, with maximum amplitude around −370 mV and −420 mV for the MM and V74M variants, respectively. At pH 8, the maximum Ni−C signal intensity corresponds to 0.3 spin/molecule in the WT, 0.25 and 0.15 spin/molecule in the MM and V74M mutants. Figure 5B shows the Ni−C spectrum at very low temperature (6 K) in conditions where the signal is split by the magnetic coupling between the NiFe active site and the reduced proximal 4Fe4S cluster.[40] The splitting of the various Ni−C lines is identical for the three enzymes, which shows that the magnetic coupling between the two interacting centers is not affected in the variants. This indicates that neither the structural arrangement of the two centers, nor the exchange coupling which is highly sensitive to the intercenter bond network, are modified by the studied mutations.

Upon irradiation of the sample at $T < 100$ K, the Ni−C EPR signal disappears and is replaced by the signal of Ni-L species (Supplementary Figure 1, Supporting Information). Depending on the experimental conditions of illumination, three different Ni−L species (Ni−L1, −L2 and −L3) could be observed,[41] the Ni−L2 species being more stable. These conversions were interpreted as resulting from the photodissociation of a hydrogenated species from the Ni−Fe site.[42] This photoprocess can be fully reversed by increasing the temperature above 120 K. We have carefully studied the kinetics of the recombination process of the Ni−L2 species into Ni−C by EPR. In the WT enzyme, this recombination process is monoexponential and the temperature dependence study of the rate constant led to an activation energy of 36 ± 3 kJ/mol (Figure 5C). In contrast, in the case of the MM mutant, a small amount of the Ni−L2 species (<0.03 spin per molecule) does not recombine even after being warmed at 200K for ten min. Furthermore, the kinetics of the Ni−L2 to Ni−C recombination is clearly heterogeneous and can be modeled as a biexponential decay. The temperature dependence of the two corresponding rate constants led to an activation energy in the MM mutant (around 20−25 kJ/mol) significantly lower than in the WT enzyme (Figure 5C). A similar behavior was observed for the V74M mutant (not shown). Thus, although the same reduced NiFe species were observed in the WT and in both mutants, our results indicate that the kinetics of the recombination process that involves proton transfer[22,41] are significantly affected by the mutations.

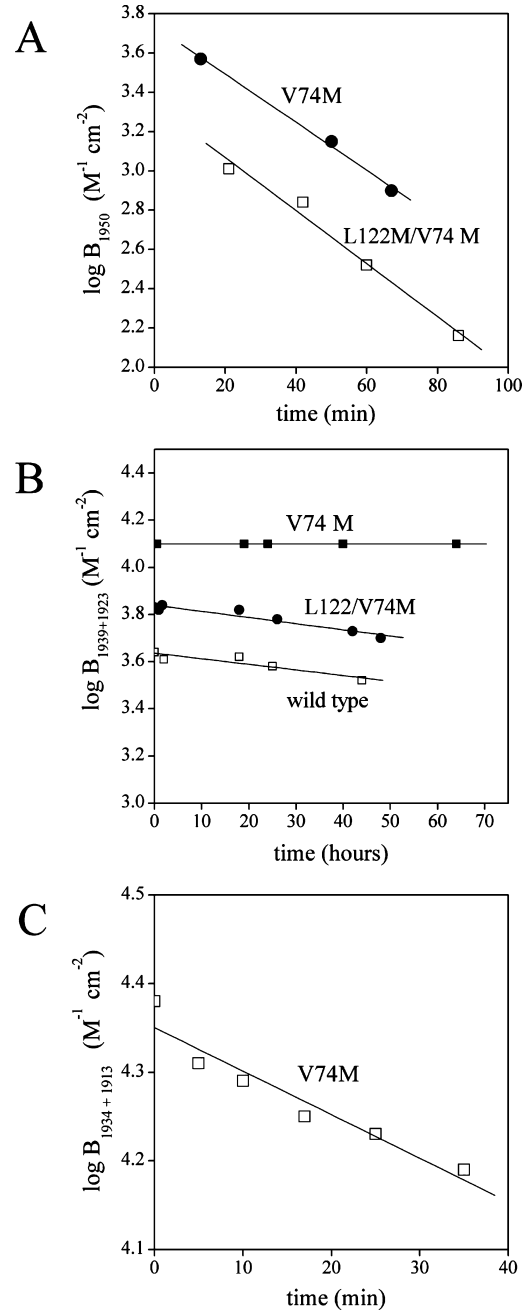

Figure 6. FTIR measurements of the activation-inactivaton kinetics. (A) Decrease of the integrated intensity of the main band (1950 cm^{-1}) of the SU state (silent unready) at an applied potential of −540 mV vs SHE in the spectroelectrochemical cell (anaerobic activation). (B) Decrease of the integrated intensity of the main bands of the Ni−R states (1939 and 1923 cm^{-1}) upon slow diffusion of air through the filling ports of a gastight transmission FTIR cell (aerobic inactivation). (C) Decrease of the integrated intensity of the CO bands of the SI states (1934 and 1913 cm^{-1}) at an applied potential of 0 mV vs SHE in the spectroelectrochemical cell (anaerobic inactivation). All experiments were done at 25 °C and pH = 8.0.

3.6. FTIR Spectroscopy. The frequencies of the bands of all states of the mutant enzymes are almost the same as for the WT enzyme in all states, which indicates that the mutations do not perturb the electron density distribution at the active site. The hydrogenase activation kinetics (Figure 6A) were determined by measuring at an applied redox potential of −540 mV vs SHE the disappearance of the silent unready Ni−SU state. This is the rate-limiting step of the activation process.[1] The

(40) Guigliarelli, B.; More, C.; Fournel, A.; Asso, M.; Hatchikian, E. C.; Williams, R.; Cammack, R.; Bertrand, P. *Biochemistry* **1995**, *34*, 4781–4790.
(41) Dole, F.; Medina, M.; More, C.; Cammack, R.; Bertrand, P.; Guigliarelli, B. *Biochemistry* **1996**, *35*, 16399–16406.
(42) Lubitz, W.; Reijerse, E.; van Gastel, M. *Chem. Rev.* **2007**, *107*, 4331–4365.

decrease of the integrated intensity of the main band at 1950 cm^{-1} led to the determination of first-order rate constants of 4.7×10^{-4} and 5.2×10^{-4} s^{-1} in the case of the M and MM mutants, respectively, compared to 2.0×10^{-4} s^{-1} for the WT enzyme under the same conditions.[43]

Inactivation processes were explored under both aerobic and anaerobic conditions. In the former case (Figure 6B), the decrease of the main bands of the Ni-R state (1939 and 1923 cm^{-1}), which predominates in the sample saturated with H_2, was measured following slow diffusion of air through the filling ports of a standard transmission cell. The Ni-R state of the active site participates in the catalytic cycle and corresponds to a fully reduced enzyme.[1] For the M mutant the oxidation of the Ni-R state was very slow, the Ni-A and Ni−B signals appearing after 200 h. For the native enzyme and the MM mutant the oxidation process was twice as fast. Anaerobic inactivation (Figure 6C) was followed by measuring the rate of conversion of the Ni−SI signal into Ni−B signal, in the absence of O_2 at a high electrode potential (0 V vs SHE). In all standard [NeFe] hydrogenases there is a kinetic barrier for this conversion.[1] Like in aerobic inactivation, the rate of anaerobic inactivation is slower for the mutants than for the WT. For the V74M mutant, the first order rate constant for the disappearance of the two Ni−SI states (measured for the CO bands at 1934 and 1913 cm^{-1}, respectively) was 1.9×10^{-4} s^{-1}, compared to 4.5×10^{-4} s^{-1} for the WT.[44]

3.7. XAS. The coordination environment and oxidation state of the Ni atom in the oxidized state (mainly Ni-A) and dithionite-reduced Ni-R state of WT, FI, V74M, and MM mutants was studied by X-ray absorption spectroscopy (XAS) at the Ni K-edge. The XAS spectra of the four proteins were rather similar (Figure 7), excluding major differences in the Ni coordination. The XANES spectra (Figure 7A) of oxidized proteins are typical for five-coordinate Ni with dominant sulfur coordination;[45] the edge energies (Supplementary Table 2, Supporting Information) suggested it was in the form of Ni (III), in agreement with the EPR data. In the reduced state, the shift of the K-edge by about 1 eV to lower energies (Supplementary Table 2, Supporting Information) was indicative of the formation of Ni (II) in the Ni-R state, again in the four proteins.

The FTs of EXAFS spectra of oxidized proteins revealed a clear contribution from a short Ni−O vector (Figure 7B, arrows). Extensive simulations of spectra under variation, e.g., of the number of Ni−S and Ni−O interactions (not shown), lead to the best-fit results which we collected in Supplementary Table 2 (Supporting Information), assuming a Ni coordination by one oxygen and four sulfur atoms. The Ni−O distance of ∼1.85 Å suggests that the O-atom belongs to a Ni−Fe bridging species (μO-(OH) in Ni-A or μO-(H) in Ni−B). The mean Ni−Fe distance of ∼2.7 Å is comparable to previous XAS[46] and crystallographic data[31,47] of the Ni-A,B states. The interatomic distances from XAS and crystallography of the oxidized V74M and MM mutants are well in agreement (Figure 4).

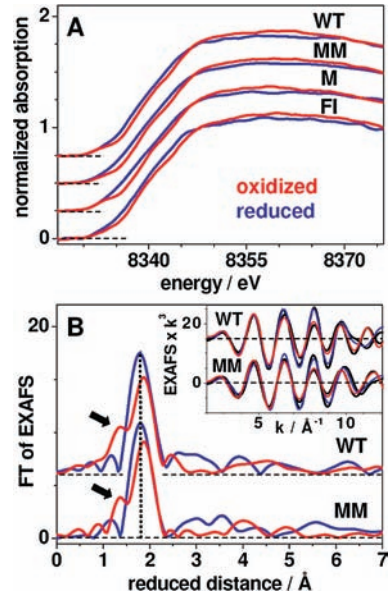

Figure 7. XAS spectra of WT and mutant proteins. (A) XANES spectra; (B) FTs of EXAFS spectra (arrows mark contributions from the O_2-ligand at Ni detected only in oxidized proteins); inset backtransforms of FTs of experimental EXAFS spectra in the range of 0.8−3.0 Å into the *k*-space (black lines) and simulations (colored lines) based on data in Supplementary Table 2 (Supporting Information).

The FTs obtained for the reduced proteins consistently revealed the loss of the peak due to the Ni−O_2 interaction (Figure 7B). On average, the short Ni−S distances were diminished by ∼0.07 Å in all four proteins (Supplementary Table 2, Supporting Information), in line with the replacement of an oxygen species in the Ni−A/B states by a hydrogen species in the Ni−C/R states. The Ni−Fe distances were reduced by ∼0.2 Å in the reduced state (to a mean value of ∼2.5 Å), in agreement with the loss of the Ni−Fe bridging oxygen species. In conclusion, the XAS data are consistent with a Ni−Fe bridging oxygen species in the oxidized state and its loss in the Ni-R state in WT and all mutant proteins.

4. Discussion

4.1. FI Mutation Has No Effect on O_2-Sensitivity. A few examples of O_2-tolerant [NiFe] hydrogenases are known.[4] Unfortunately, these enzymes are not well-suited for biohydrogen applications because they are not highly active and they cannot be expressed in an active form in heterologous hosts.[48] However, they may provide valuable models for studies on resistance mechanisms to O_2 inhibition. Based on the "molecular sieve" hypothesis inspired by sequence comparison with O_2-insensitive H_2 sensors,[15] we constructed the *D. fructosovorans* [NiFe] hydrogenase V74I/L122F (FI) mutant to test whether these changes would increase its O_2 tolerance. Although the double mutation reduces the diameter of the gas channel and the rate of intramolecular diffusion, which increases the Michaelis constant for H_2 5-fold,[14] it does not provide any tolerance

(43) De Lacey, A. L.; Pardo, A.; Fernandez, V. M.; Dementin, S.; Adryanczyk-Perrier, G.; Hatchikian, E. C.; Rousset, M. *J. Biol. Inorg. Chem.* **2004**, *9*, 636–642.
(44) de Lacey, A. L.; Fernandez, V. M.; Rousset, M.; Cavazza, C.; Hatchikian, E. C. *J. Biol. Inorg. Chem.* **2003**, *8*, 129–134.
(45) Colpas, G. J.; Maroney, M. J.; Bagyinka, C.; Kumar, M.; Willis, W. S.; Suib, S. L.; Mascharak, P. K.; Baidya, N. *Inorg. Chem.* **1991**, *30*, 920–928.
(46) Gu, Z.; Dong, J.; Allan, C. B.; Choudhury, S. B.; Franco, R.; Moura, J. J. G.; Moura, I.; LeGall, J.; Przybyla, A. E.; Roseboom, W.; Albracht, S. P. J.; Axley, M. J.; Scott, R. A.; Maroney, M. J. *J. Am. Chem. Soc.* **1996**, *118*, 11155–11165.
(47) Ogata, H.; Hirota, S.; Nakahara, A.; Komori, H.; Shibata, N.; Kato, T.; Kano, K.; Higuchi, Y. *Structure (Camb)* **2005**, *13*, 1635–1642.
(48) Böck, A.; King, P. W.; Blokesch, M.; Posewitz, M. C. Maturation of hydrogenases in *Adv. Microb. Physiol.* **2006**, *51*, 1−71.

to O_2 (Figures 2A and 3). Recently, the same single and double mutations were performed in the MBH enzyme from *R. eutropha*.[49] The FI mutant exhibited a 100 fold increased $K_M(H_2)$ compared to the WT enzyme and was apparently more sensitive to O_2 (the apparent O_2-inhibition constant decreased from 1000 to 260 μM). However, the fact that gas diffusion was slowed 10-fold in the *D. fructosovorans* FI mutant[14] led us to conclude that these positions close to the active site could play a role in O_2 tolerance if V74 and L122 were replaced by other amino acids.

4.2. Methionines Provide O_2-Tolerance. The choice of methionine came from the affinity of their sulfur atom for oxygen, which results in a strong reactivity with reactive oxygen species (ROS) as it occurs in oxidative stress response,[18,19] or in the ability to form weak S−O interactions.[21] We made the hypothesis that methionines placed at the entrance of the active site cavity at positions M74 and M122 may protect the Ni−Fe site from oxidation, either by reacting or at least by interacting with the oxygen species present at the active site under oxidizing conditions.[31] In the first case, MetSO would be formed, which might subsequently be reduced by the electrons supplied by the active site through a concomitant oxidation of the nearby Ni-cysteine ligand C543 known to be flexible,[3] following a mechanism similar to that of methionine sulfoxide reductases.[50] Alternatively, the ability of methionine to engage weak S−O bonds[21] might facilitate the evacuation of the bound oxygen species from the active site.

To test our hypothesis, we constructed the [NiFe]-hydrogenase V74M and L122 M mutants and the double V74M/L122 M mutant. The V74M mutation is the closest to the active site. We studied hydrogenase oxidation kinetics in the presence of O_2 using two methods: PFV[25,26] and HDE.[51] Using these techniques, we clearly show that the MM and V74M mutated hydrogenases became O_2 tolerant (Figures 2, 3 and 4), meaning that the enzymes remain active when exposed for several minutes to high O_2 concentrations. HDE revealed that the presence of MV further increased O_2 tolerance, as the V74M mutant is able to consume D_2 in the presence of 150 μM of O_2 (Figure 2B), which is close to the O_2 concentration of 200 μM measured in air-equilibrated solutions. Under these conditions, the activity is about 10% of the activity measured in anaerobiosis. These results indicate that in the presence of MV, approximately 10% of the enzyme population remains active, in dynamic equilibrium with an inactive oxidized, easily reactivated fraction. On the other hand, an interesting property of the MM mutant was detected by PFV: unlike the WT enzyme, it partly reactivates in the presence of H_2 even under very oxidizing conditions (Figure 3), in a process that is distinct from the usual reactivation that results from reducing the enzyme. The M mutant also reactivates under H_2 at high potential but to a lesser extent (Figure 3 and ref 39). This reactivation property is probably related to the slower kinetics of anaerobic inactivation of mutant M compared to the WT enzyme (Figure 6C). These results clearly show that the mutated hydrogenases acquired important resistance properties to O_2 inhibition, which supports our hypothesis regarding the protective function of methionine side chains.

4.3. Methionines are Not Oxidized. To check whether oxygenated forms of C543 or M74 are actually produced, we solved the X-ray structure of the methionine mutants in the oxidized state. The analysis of both V74M (Figure 4A) and MM mutant (Figure 4B, ref 14) structures indicated the formation of oxidized species similar to WT, presumably corresponding to a mixture of Ni-A and Ni−B states, in agreement with the major spectral components observed by EPR (Figure 5A). Neither sulfenate nor methionine sulfoxide were observed in the oxidized enzyme preparations, which better support the mechanism of the facilitated extraction of the oxygen species. However, we cannot exclude that such oxidized species are formed but are too short-lived to be observed in the crystals.

4.4. Methionines Have a Kinetic Effect. To get a better view on the mechanism, we studied by FTIR and EPR spectroscopy the redox states of the active site and we also analyzed by XAS the atomic species bound to Ni. XAS studies showed that the ligands of the Ni ion were similar in the mutants and the native enzyme, both in the oxidized and fully reduced states (Figure 7), which suggests that the mutations do not modify the catalytic mechanism. Both EPR and FTIR spectroscopy indicated that the usual Ni species were present, but also revealed significant differences that are likely to influence the reactivity of the mutants. From EPR data it is possible to deduce that the presence of methionine may have altered the hydrogen-bonding network near the active site in the reduced state, as suggested by the lower activation energy of the Ni-L2 recombination process (Figure 5C). This observation reveals that methionine interacts with the active site and modifies its environment. FTIR showed that the mutants were inactivated more slowly and reactivated more rapidly than the native enzyme (Figure 6). The slower rate of oxidation of the active site's Ni-R state observed in presence of air for the M mutant may in part explain the activity of the enzyme in the presence of dioxygen (Figure 2B).

4.5. Interaction of Peroxide with Methionines Facilitates its Protonation. The slower inactivation is attributed to a reduced active site accessibility that is due to partial tunnel obstruction by the mutations.[14] The faster activation of inactive enzyme however, necessarily involves a quicker removal of the bound peroxide (OOH^-). If this leaves the active site as HOOH, it first needs to be protonated at the Ni−Fe bridging O-atom. The latter would be expected to be a much better proton acceptor if its bond to the iron is broken by moving to the terminal Ni ligation site. Modeling shows that in this conformation, with the first O-atom at 2 Å from the Ni, there is space for the second O-atom to sit at about 3.2 Å from M74Sδ (Figure 8). The terminal methyl group of the methionine is positioned approximately on the same line on the other side of the Sδ, opposite the O-atom. This conformation resembles the observed binding mode of the competitive CO inhibitor[52] and gives the correct geometry for a weak S···O interaction, as observed in statistical analyses of preferred contacts of divalent sulfur atoms with nucleophiles, both in small compounds[53] and in protein structures.[21] After protonation of the Ni-bound O-atom through E25 and Cys543Sγ,[22] the resulting H_2O_2 molecule could leave the Ni and move around the M74Sδ atom, assisted by weak nucleophilic (from O) and/or electrophilic (from H) interactions with it and by dynamic movements of the protein. Accordingly,

(49) Ludwig, M.; Cracknell, J. A.; Vincent, K. A.; Armstrong, F. A.; Lenz, O. *J. Biol. Chem.* **2009**, *284*, 465–477.
(50) Boschi-Muller, S.; Gand, A.; Branlant, G. *Arch. Biochem. Biophys. Special Issue: Enzymology in Europe* **2008**, *474*, 266–273.
(51) Berlier, Y.; Lespinat, P. A.; Dimon, B. *Anal. Biochem.* **1990**, *188*, 427–431.
(52) Ogata, H.; Mizoguchi, Y.; Mizuno, N.; Miki, K.; Adachi, S.; Yasuoka, N.; Yagi, T.; Yamauchi, O.; Hirota, S.; Higuchi, Y. *J. Am. Chem. Soc.* **2002**, *124*, 11628–11635.
(53) Rosenfield, R. E.; Parthasarathy, R.; Dunitz, J. D. *J. Am. Chem. Soc.* **1977**, *99*, 4860–4862.

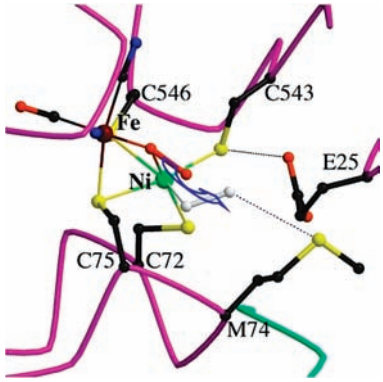

Figure 8. Mechanism proposed for the activation of the V74M mutant in the unready state. The role of M74 in the stabilization of a proposed transition state with terminally bound peroxide is shown in white. The peroxide bound to the active site in the unready enzyme[31] is shown in red. The arrow indicates its proposed rearrangement toward the terminal Ni-ligation site opposite to Cys546.

in addition to stabilizing the terminally bound peroxide, Met74 may also provide an assisted escape route for H_2O_2 toward the gas channel (Figure 1).

5. Conclusion

The complexity of the system studied made necessary the association of a large number of techniques to get a picture as detailed as possible of the mechanisms in action. The sum of our results indicates that the methionines do not modify the catalytic mechanism but rather influence the reactivity of the enzyme with O_2, mainly at the kinetic level. The slower inactivation by O_2 is attributed to a more restricted active site accessibility that is due to partial tunnel obstruction by the mutations. An additional protective role of M74 residues such as that related to a direct oxidation and transient formation of MetSO remains a possibility.

Furthermore, the facilitated enzyme activation in the M mutants must be related to a decrease of the energy of the transition states that are involved in this process. We propose that M74 stabilizes the rearrangement of the peroxide species that is necessary to allow its protonation through E25 and C543, before its escape from the oxidized enzyme. Similarly, it could favor the escape of a water molecule needed for the activation of ready enzymatic states.

In this study, we have demonstrated for the first time that it is possible to induce O_2-tolerance in a [NiFe] hydrogenase, in such a way that modified enzymes are active in the presence of O_2 at concentrations close to that in air-equilibrated solutions. The fact that methionine substitutions are located in conserved regions makes it possible to engineer [NiFe] hydrogenases in a wide range of organisms, as heterologous expression of [NiFe] hydrogenase is difficult. This achievement opens the way for future development in the field of biological hydrogen production or utilization.

Acknowledgment. This work was funded by the CNRS, CEA, ANR, ACI-ECD110, the University of Provence, the City of Marseilles, and supported by the *Pôle de compétitivité Capénergies.* M.H. thanks Unicat CoE Berlin, EU-SolarH2, and DFG-SFB498-C8 for financial support. V.F. and A.L. thank the Spanish MEC (project CTQ2006-12097) for financial support.

Supporting Information Available: Crystallographic data for the V74M structure are presented in Supplementary Table 1, Nickel EXAFS fit parameters and K-edge energies are presented in Supplementary Table 2 and the biphasic kinetics of the Ni−C EPR signal appearance during the Ni−L2 to Ni−C recombination process is presented in Supplementary Figure 1. This material is available free of charge via the Internet at http://pubs.acs.org.

JA9018258